Title

RGS10 physically and functionally interacts with STIM2 and requires store-operated calcium entry to regulate pro-inflammatory gene expression in microglia

Authors

Wendimu, Menbere Y
Alqinyah, Mohammed
Vella, Stephen
et al.

Publication Date

2021-07-01

DOI

10.1016/j.cellsig.2021.109974

Peer reviewed

HHS Public Access

Author manuscript

Cell Signal. Author manuscript; available in PMC 2022 July 01.

Published in final edited form as:

Cell Signal. 2021 July ; 83: 109974. doi:10.1016/j.cellsig.2021.109974.

RGS10 physically and functionally interacts with STIM2 and requires store-operated calcium entry to regulate proinflammatory gene expression in microglia

Menbere Wendimu[1], **Mohammed Alqinyah**[1,#], **Stephen Vella**[2], **Phillip Dean**[1], **Faris Almutairi**[1], **Roseanne Davila Rivera**[1], **Shima Rayatpisheh**[3], **James Wohlschlegel**[3], **Silvia Moreno**[2], **Shelley B. Hooks**[1,*]

[1]Department of Pharmaceutical and Biomedical Sciences, University of Georgia, Athens, GA 30602

[2]Department of Cellular Biology, University of Georgia, Athens, GA 30602

[3]Department of Biological Chemistry, University of California, Los Angeles 90095

Abstract

Chronic activation of microglia is a driving factor in the progression of neuroinflammatory diseases, and mechanisms that regulate microglial inflammatory signaling are potential targets for novel therapeutics. Regulator of G protein Signaling 10 is the most abundant RGS protein in microglia, where it suppresses inflammatory gene expression and reduces microglia-mediated neurotoxicity. In particular, microglial RGS10 downregulates the expression of pro-inflammatory mediators including cyclooxygenase 2 (COX-2) following stimulation with lipopolysaccharide (LPS). However, the mechanism by which RGS10 affects inflammatory signaling is unknown and is independent of its canonical G protein targeted mechanism. Here, we sought to identify non-canonical RGS10 interacting partners that mediate its anti-inflammatory mechanism. Through RGS10 co-immunoprecipitation coupled with mass spectrometry, we identified STIM2, an endoplasmic reticulum (ER) localized calcium sensor and a component of the store-operated

*To whom correspondence should be addressed: Shelley B. Hooks: Department of Pharmaceutical and Biomedical Sciences, University of Georgia Athens, GA 30602; shooks@uga.edu; Tel. (706)542-2189; Fax (706)54222-5358.

#:Present address: Department of Pharmacology and Toxicology, King Saud University

CRediT Authorship Contributions

Menbere Wendimu:
Conceptualization, Data Curation & Analysis, Manuscript Writing- Original Draft, Review & Editing

Mohammed Alqinyah:
Conceptualization, Data Curation & Analysis, Manuscript Writing- Review & Editing

Stephen Vella, Faris Almutairi, Roseanne Rivera, Phillip Dean, Shima Rayatpisheh:
Data Curation & Analysis

James Wohlschlegel & Silvia Moreno:
Conceptualization

Shelley B. Hooks:
Conceptualization, Data Analysis, Funding Acquisition, Project Supervision, Manuscript Writing- Review & Editing

Declarations of Interest

The authors declare that they have no conflicts of interest with the contents of this article.

calcium entry (SOCE) machinery, as a novel RGS10 interacting protein in microglia. Direct immunoprecipitation experiments confirmed RGS10-STIM2 interaction in multiple microglia and macrophage cell lines, as well as in primary cells, with no interaction observed with the homologue STIM1. We further determined that STIM2, Orai channels, and the Ca^{2+-}-dependent phosphatase calcineurin are essential for LPS-induced COX-2 production in microglia, and this pathway is required for the inhibitory effect of RGS10 on COX-2. Additionally, our data demonstrated that RGS10 suppresses SOCE triggered by ER calcium depletion and that ER calcium depletion, which induces SOCE, amplifies proinflammatory genes. In addition to COX-2, we also show that RGS10 suppresses the expression of proinflammatory cytokines in microglia in response to thrombin and LPS stimulation, and all of these effects require SOCE. Collectively, the physical and functional links between RGS10 and STIM2 suggest a complex regulatory network connecting RGS10, SOCE, and pro-inflammatory gene expression in microglia, with broad implications in the pathogenesis and treatment of chronic neuroinflammation.

Keywords

Regulator of G protein Signaling (RGS)10; microglia; neuroinflammation; store-operated calcium entry (SOCE); toll-like receptor (TLR); stromal interaction molecule (STIM)2; cyclooxygenase (COX)-2

1. Introduction

Chronic inflammation is an underlying mechanism for the initiation and progression of multiple diseases[1]. Chronic activation of microglia cells is a driving factor of neuroinflammation and a hallmark of several neurodegenerative diseases including Parkinson’s disease, Alzheimer’s disease, and Multiple Sclerosis [2]. Aberrant activation of microglia leads to amplified production of proinflammatory cytokines, prostaglandins, and other neurotoxic molecules, ultimately contributing to neuroinflammation and neurotoxocity[2, 3]. Therefore, targeting novel molecular mechanisms for the regulation of microglial inflammatory signaling is a promising therapeutic strategy for neurodegenerative diseases.

Regulator of G protein Signaling 10 (RGS10) is the most abundant RGS protein in microglia, where it exerts anti-inflammatory and neuroprotective effects [4-7]. A series of studies by Lee et al. [6, 7] demonstrated that RGS10 knockout mice display significantly more activated microglia and higher levels of inflammatory cytokines. Further, loss of RGS10 exacerbates inflammation-induced toxicity of dopaminergic neurons, suggesting a neuroprotective role of RGS10[5-7]. This anti-inflammatory role of RGS10 is also observed and consistently modeled in BV2 microglia, a suitable cellular model for neuroinflammation studies[8]. We and others have shown that loss of RGS10 in BV2 microglia cells enhances the expression of various pro-inflammatory cytokines in response to toll-like receptor 4 (TLR4) activation[4, 6, 7, 9]. In particular, RGS10 downregulates Lipopolysaccharide (LPS)-stimulated expression of multiple pro-inflammatory genes, including a profound negative regulation of the inflammatory kingpin cyclooxygenase-2 (COX-2) and its primary metabolic product Prostaglandin E2 (PGE2)[4].

RGS proteins canonically act as GTPase accelerating proteins (GAPs) for heterotrimeric G proteins and inhibit signaling initiated by G protein-coupled receptors; this GAP function is mediated through interaction with activated G protein subunit[10, 11]. However, the mechanism by which RGS10 affects LPS-induced pro-inflammatory gene expression is independent of its canonical G protein targeted mechanism and does not require G protein interaction [4]. This suggests that novel RGS10 interacting partners may account for its effect on regulating LPS/TLR4 proinflammatory signaling. The goal of this study was to identify and validate non-canonical microglial RGS10 interacting partners that may mediate the anti-inflammatory functions of RGS10. Here, we describe a novel interaction between RGS10 and stromal interaction molecule 2 (STIM2) and establish STIM2 as an important regulator of LPS-induced inflammatory gene expression in microglia. STIM2 is an endoplasmic reticulum (ER) calcium sensor which detects ER calcium depletion and triggers store-operated calcium entry (SOCE) via activation of plasma membrane Orai channels[12-14]. This study characterizes the physical and functional interaction of RGS10 and STIM2 and defines the role of the SOCE pathway on RGS10's anti-inflammatory function.

2. Results

2.1. RGS10 interaction partners in microglia

We previously demonstrated that RGS10 regulates inflammatory gene expression in microglia through a G protein-independent mechanism [4]. To identify RGS10 interacting proteins that may mediate this activity, wildtype BV-2 cell total cell lysates were immunoprecipitated with either control IgG or RGS10 antibody, and retained proteins were eluted and analyzed. Robust and selective RGS10 pulldown was observed, with no detectable RGS10 immunoreactivity remaining in the supernatant following immunoprecipitation (IP), and no detectable RGS10 precipitating with control IgG. RGS10 immunoreactivity was fully recovered in a single round of elution (Figure S1A). The elution fractions were subjected to protease digestion and reversed-phase separation coupled to tandem mass spectrometry. As expected, we identified strong RGS10 enrichment along with the classic RGS interacting proteins guanine nucleotide-binding protein subunits Gαi2 and Gαi3. In addition to the canonical G protein partners, we identified 23 proteins that were specifically enriched in RGS10 co-IP compared to control IgG pulldown with a SAINT score of 0.8 or higher (Table S1). Consistent with previous reports of RGS10 distribution throughout the cytoplasm and nucleus[15], more than half of the interacting proteins are localized in these two compartments (Figure S1B). To validate the data obtained from LC-MS/MS analysis, we conducted direct co-IP experiments probing for select individual proteins, including Gαi3, STIM2, Syntaxin 5, and PDE4A (Figure S1C). These results indicate that endogenous RGS10 physically interacts—directly or indirectly—with multiple non-classic binding partners in BV2 microglia, suggesting potentially diverse, non-canonical roles for RGS10.

2.1.2. RGS10-STIM2 interaction—Of the potential novel RGS10-interacting proteins, STIM2 was of particular interest because of its prominent role in Ca^{2+} signaling in immune cells and its implicated role in regulating inflammatory responses in microglia and

macrophages [16-18]. In particular, STIM2 in macrophages facilitate LPS-induced production of multiple pro-inflammatory genes in macrophages, including TNFα, IL-6, and IL-1β[18], and these cytokines are also known to be regulated by RGS10 in microglia[4, 6, 9]. To characterize RGS10 interaction with STIM2, we first assessed the specificity of the co-immunoprecipitation experiment. We performed RGS10 immunoprecipitation (IP) in RGS10-null BV2 microglia in which RGS10 expression has been disrupted using CRISPR ($RGS10^{-/-}$) and in control CRISPR BV2 cells (control) which express a normal level of endogenous RGS10 [4] using both RGS10 and control IgG antibodies. We observed no STIM2 or RGS10 immunoreactivity precipitating with RGS10 antibody in knockout lysates, or with control IgG in control lysates, thereby ruling out non-specific immunoprecipitation (Figure 1A). We also observed RGS10-STIM2 co-immunoprecipitation (co-IP) in N9 microglia and RAW264.7 macrophage cell lines, and in primary mouse peritoneal macrophages (Figure 1B). Collectively, these data suggest that endogenous RGS10 specifically interacts with STIM2 *in vitro* and in primary immune cells.

STIM2 shares approximately 50% identity with its homolog STIM1[19], which is also expressed in microglia and is implicated in the regulation of inflammatory signaling [17, 20], suggesting a possible interaction of RGS10 with STIM1. However, STIM1 was not identified as an interacting protein in our proteomics results or direct RGS10 co-IP (Table S1 & Figure 1C), indicating that RGS10 selectively associates with STIM2. In addition to binding calcium ions directly, STIM2 also binds the calcium-binding regulatory protein calmodulin (CaM) [21], and a Ca^{2+}-dependent interaction between RGS10 and CaM has been reported in other cellular models [22, 23]. Therefore, we predicted that CaM may serve as a bridge between RGS10 and STIM2 to facilitate Ca^{2+}-dependent interaction in microglia. To examine this, we tested whether CaM co-precipitates with RGS10 in BV2 cells and if Ca^{2+}-CaM regulates the RGS10-STIM interaction. We did not observe a difference in the extent of RGS10-STIM2 interaction in co-IP assays performed in the presence of excess calcium or the calcium chelator EGTA, while STIM1 did not co-IP with RGS10 under the conditions tested (Figure 1D). We also did not detect an interaction between RGS10 and CaM under these conditions, regardless of calcium level. These results suggest that RGS10 interaction with STIM2 does not require calcium or calmodulin. Immunoprecipitations for proteomics analysis and experiments shown in Figures 1A-D were performed on total cell lysates containing sodium deoxycholate (SDC), while previous studies that detected RGS10-CaM interaction were performed in the absence of this detergent[23]. We confirmed Ca^{2+}-dependent RGS10 interaction with CaM in BV2 cell lysates prepared with lower stringency co-IP buffer lacking SDC (Figure 1E). Our results collectively suggest a robust, calcium-insensitive interaction between RGS10 and STIM2, and a detergent-sensitive, Ca^{2+}-dependent interaction between RGS10 and CaM.

Given that RGS10 suppresses inflammatory signaling triggered by TLR4 activation, we next determined whether RGS10-STIM2 interaction in microglia is regulated by LPS. We compared RGS10-STIM2 co-IP in resting BV2 cells or cells activated by LPS for 3 hours, a time point that corresponds to the initiation of LPS stimulated expression of proinflammatory mediators[24, 25]. We did not observe a difference in RGS10-STIM2 interaction in co-IP experiments, suggesting that the interaction of RGS10 and STIM2 is not

impacted by LPS stimulation at this time point (Figure 1F), although it remains possible that LPS triggers a transient change in this interaction.

2.2. Role of STIM2 and Orai-Calcineurin pathway in COX-2 regulation

Previous studies have implicated the role of STIM2 in regulating inflammatory signaling[18, 26]. In particular, Sogkas *et al.* [18] showed that STIM2 knockout mice are resistant to LPS-induced inflammation *in vivo* and that primary macrophages isolated from STIM2 knockout mice display impaired TLR-4 induced expression of pro-inflammatory genes. STIM2 facilitates migration and phagocytosis of microglia in response to extracellular nucleotide[17], but its role in regulating microglial inflammatory responses has not been explored. Here, we examined the effect of STIM2 on the inflammatory signaling events that are modulated by RGS10, in particular the regulation of COX-2 by TLR4 activation. COX-2 expression is highly inducible in response to inflammatory stimuli including the bacterial epitope LPS [27, 28]. We show that transient transfection of STIM2 siRNA in BV2 cells resulted in greater than 75% reduction of STIM2 protein levels and inhibited LPS-induced COX-2 protein by approximately 50%, indicating that STIM2 is required for maximal LPS stimulated COX-2 expression (Figure 2A-C). STIM2 siRNA did not affect the expression of the STIM homologue STIM1, ruling out an off-target effect (Figure S2). LPS treatment suppressed RGS10 expression as we and others have previously reported [4, 9], but it caused a marked increase in STIM2 protein level (Figure 2A&B). These results suggest that STIM2 facilitates LPS-stimulated COX-2 expression.

The established role of STIM proteins is to serve as a sensor for endoplasmic reticulum (ER) Ca^{2+} store depletion and to couple this depletion to extracellular Ca^{2+} entry through activation of plasma membrane Orai channels, a mechanism known as store-operated calcium entry (SOCE) [29, 30]. Orai channels are strongly coupled to the activation of the Ca^{2+}-dependent phosphatase calcineurin and downstream targets which regulate calcium-dependent inflammatory gene expression [16, 31-34]. To define the role of the Orai-calcineurin function in regulating LPS response, we examined LPS-induced COX-2 gene expression following pharmacologic inhibition of either Orai using YM58483 (YM), or calcineurin using cyclosporin A (CsA). Inhibition of either Orai channels or calcineurin significantly blocked LPS-induced COX-2 production in BV2 microglia (Figure 2D), suggesting that the SOCE pathway is essential for COX-2 production in response to TLR4 activation. To validate whether this pathway mediates a similar function in other cell lines, we examined the effect of YM and CsA on LPS-induced COX-2 expression in N9 cells, an alternative immortalized cell line (Figure 2E). We observed a similar effect in N9 cells in which YM and CsA significantly reduced COX-2 expression. In addition to BV2 and N9 cells, we also confirmed our result in primary microglia in which Orai inhibition blocked LPS-induced COX-2 transcript levels (Figure 2F). Altogether, our data suggest that components of the SOCE pathway, including STIM2, Orai, and calcineurin, are essential for LPS-induced COX-2 production.

2.3. Impact of STIM2 and Orai-Calcineurin signaling axis on RGS10 sensitive COX-2 expression.

The observed effect of STIM2 expression and Orai/calcineurin activity on LPS-stimulated COX-2 expression contrasts our previous observation that loss of RGS10 expression upregulates LPS-induced COX-2[4]. This opposing effects of STIM2 and RGS10 on LPS signaling, along with the observed biochemical interaction, suggested a potential functional link between RGS10 and STIM2. To determine the role of STIM2 in RGS10-sensitive COX-2 expression, we performed STIM2 knockdown in Control and RGS10$^{-/-}$ BV2 cells. STIM1, STIM2, and Orai protein levels were unchanged in RGS10$^{-/-}$ cells (data not shown). As expected, LPS-induced COX-2 expression was enhanced in RGS10$^{-/-}$ cells compared to control cells as expected, but this upregulation was significantly inhibited by STIM2 knockdown (Figure 3A-C). In cells with STIM2 knockdown, loss of RGS10 did not significantly enhance LPS-stimulated COX-2 expression. Similarly, the observed upregulation of COX-2 mRNA and protein in RGS10 knockout cells was inhibited in the presence of either the Orai inhibitor YM (Figure 3D&E) or the calcineurin inhibitor CsA (Figure 3F&G). Collectively, our data demonstrate that the STIM2-Orai-calcineurin pathway is required for RGS10-mediated regulation of LPS-induced COX-2 production.

2.4. Effect of calcium store depletion on LPS stimulated COX-2 expression.

Since the SOCE pathway is activated following ER Ca^{2+} store depletion[29, 30], we examined whether ER calcium depletion itself affects LPS-induced COX-2 production. We pretreated BV-2 cells with the SERCA-Ca^{2+}-ATPase inhibitor Thapsigargin (TG) to trigger ER calcium depletion prior to LPS stimulation and examined its effect on transcript and protein levels of COX-2 and RGS10. A short-term (20 min) pretreatment with TG before LPS (PreTG) enhanced LPS-mediated induction of COX-2 transcript and protein levels more than fivefold over the effect seen with LPS alone (Figure 4A & B). TG pre-treatment also enhanced LPS-induced downregulation of RGS10 protein level (Figure 4A), suggesting that ER calcium depletion amplifies positive regulation of COX-2 and negative regulation of RGS10 expression in response to LPS. To delineate whether the TG-induced transient calcium elevation or the secondary SOCE response is responsible for enhancing LPS-stimulated COX-2 expression, we co-treated cells with LPS and either the Orai inhibitor (YM) or the calcineurin inhibitor (CsA), following TG pretreatment. Both YM and CsA significantly suppressed TG-mediated upregulation of LPS-induced COX-2 expression (Figure 4C), indicating that the effect of thapsigargin on COX-2 expression is dependent on the SOCE pathway. Altogether, these results suggest that the STIM2-Orai-calcineurin mediated SOCE pathway, which is triggered by ER depletion, amplifies LPS-stimulated COX-2 expression.

2.5. SOCE effect in RGS10-regulated pro-inflammatory genes

Although we focused on COX-2 as a known target of RGS10 regulation, both RGS10 and STIM2 also regulate other pro-inflammatory cytokines in response to LPS[4, 6, 9, 18]. To examine the dual effect of RGS10 and SOCE on additional genes, we analyzed the effect of Orai inhibitor on tumor-necrosis factor-alpha (TNFα), interleukin-6 (IL-6), and inducible nitric oxide synthase (iNOS) expression in BV2 cells after treatment with different LPS

doses (1 ng/mL and 10 ng/mL). Similar to the effect for COX-2 (Figure S3A), loss of RGS10 enhanced LPS-induced TNFα and IL-6 transcripts at both LPS doses tested, and this upregulation was blunted by Orai inhibition (Figure 5A & B). Similar regulation of iNOS expression was observed, but only at the lower LPS dose (Figure S3B). To further validate the role of SOCE on RGS10 function, we performed similar experiments in primary microglia isolated from wild type and RGS10 knockout mice. As expected, RGS10 transcript was depleted in RGS10 knockout primary microglia compared to wild type cells, and LPS suppressed RGS10 transcript in cells expressing RGS10 (Figure 5C). Consistent with our BV2 data, we observed that primary microglia lacking RGS10 had greater LPS-stimulated COX-2 and IL-6 expression, and this effect was fully inhibited in the presence of Orai inhibitor (Figure 5D & E). Orai inhibition also significantly inhibited TNFα expression in RGS10 knockout primary microglia, although the upregulation of TNFα in RGS10 knockout primary microglia compared to wildtype cells was not significant (Figure 5F). Altogether, these data suggest that RGS10 regulates LPS-stimulated pro-inflammatory gene expression in microglia through a mechanism that requires SOCE.

2.6. RGS10 and SOCE role in thrombin signaling

LPS is a commonly used stimulus to model neuroinflammation associated with neurodegeneration[35, 36], but multiple other mediators are implicated in mediating inflammation in the context of CNS injury. To explore responses associated with CNS injury, we examined the role of RGS10 and SOCE in pro-inflammatory responses of microglia to thrombin, a physiologically relevant endogenous stimulus[37]. We observed significant upregulation of COX-2, TNFα, and IL-6 transcript expression in RGS10 knockout BV2 cells compared to control cells in response to thrombin treatment (Figure 6A-C). Similar to the effect observed for LPS, the Orai-inhibitor restored RGS10 loss-mediated upregulation of COX-2 and IL-6 expression (Figure 6A & B). Orai inhibition also significantly suppressed thrombin-induced TNFα expression in RGS10 knockout cells, yet it did not fully restore TNFα upregulation (Figure 6C). We also observed a similar trend for iNOS transcript, yet the effect of both RGS10 and Orai was not statistically significant (data not shown). Overall, our results suggest that RGS10 regulates thrombin-stimulated pro-inflammatory gene expression in BV2 microglia through a mechanism involving SOCE.

2.7. RGS10 effect on store-operated calcium entry (SOCE)

Given the opposing involvement of the STIM2/SOCE pathway in mediating RGS10-sensitive pro-inflammatory gene expression, we hypothesized that RGS10 may also regulate store-operated calcium entry. To evaluate the role of RGS10 in SOCE, we conducted live cell calcium imaging of control and RGS10$^{-/-}$ BV2 cells loaded with the fluorescent Ca^{2+} indicator Cal-520-AM. A transient rise in cytoplasmic calcium was triggered upon ER calcium depletion using thapsigargin (TG) in the absence of extracellular calcium. Following a return to baseline cytoplasmic calcium levels, extracellular Ca^{2+} was added to allow store-operated calcium entry (SOCE) (Figure 7A and B). Compared to control BV2 cells, RGS10$^{-/-}$ cells displayed a reduced initial TG-induced calcium transient, while the SOCE peak was significantly enhanced (Figure 7B and C). This resulted in a SOCE:TG peak height ratio of 1.1 for control cells and 2.0 for RGS10$^{-/-}$ cells. This suggests a closer coupling of ER calcium depletion and extracellular calcium entry in the absence of RGS10

compared to control cells, and the ability of endogenous RGS10 to blunt extracellular calcium entry in response to ER calcium depletion.

3. Discussion

Chronic activation of microglia is a driving factor in the progression of neuroinflammatory diseases[2], and mechanisms that regulate microglial inflammatory signaling are potential targets for novel therapeutics[38, 39]. The small Regulator of G-protein Signaling 10 protein (RGS10) impacts the pathophysiology of diverse diseases[40], as demonstrated in various animal and cellular disease models[6, 23, 41-46]. Among these broad effects, the role of RGS10 in microglia stands out as the most pronounced and most clearly tied to pathology. Specifically, microglial RGS10 suppresses the expression of multiple pro-inflammatory genes, including a particularly profound negative regulation of COX-2 and other pro-inflammatory cytokines downstream of LPS/TLR4 activation[4, 6, 7]. While RGS10 holds great promise as an anti-inflammatory drug target, its mechanism of action is mediated through an unknown G protein-independent mechanism [4].

In this study, we identified a non-canonical interaction of microglial RGS10 with STIM2, an ER-resident calcium sensor and component of the store-operated calcium entry (SOCE) machinery[12, 13, 47]. Our collective findings revealed a bi-directional and opposing regulation of LPS-stimulated inflammatory gene expression by RGS10 and STIM2. The regulation of inflammatory gene expression is mediated by multiple pathways and components[48-53]. Recently, a direct link between LPS signaling and store-operated calcium entry has been explored in microglia. Mizuma and colleagues[54] demonstrated that LPS induces SOCE in BV2 cells, and inhibition of SOCE suppresses downstream inflammatory responses including the activation of NF_kB and NFAT, suggesting the importance of microglial SOCE to LPS signaling. Our data extend this finding to implicate STIM2, Orai, and calcineurin in facilitating LPS-stimulated response and in mediating RGS10-sensitive pro-inflammatory gene expression. In particular, we demonstrated the requirement of the STIM2-Orai-Calcineurin signaling axis for RGS10-mediated regulation of COX-2 expression in response to LPS. We also determined that the upstream trigger of SOCE, the depletion of store calcium, amplifies the pro-inflammatory effect of LPS. Additionally, our results revealed a new role of RGS10 in the regulation of SOCE triggered by store depletion. Collectively, our data demonstrate a complex signaling network linking LPS, RGS10, and SOCE which suggests that the ability of RGS10 to form a complex with and/or modulate the activity of the store calcium machinery may account for its G protein-independent anti-inflammatory effects (Figure 8).

Similar to RGS10-mediated modulation of COX-2, RGS10 also regulated LPS-induced expression of IL-6, TNFα, and to a lesser extent iNOS, in a mechanism that requires SOCE. Multiple receptor stimuli can trigger both calcium depletion from the ER and inflammatory gene expression [55]. Therefore, the ability of RGS10 to regulate SOCE may impact pro-inflammatory responses downstream of different stimuli besides the TLR4 agonist LPS, in particular regulation of pathways that converge with SOCE. Previous reports showed that the endogenous agonist thrombin elicits cytoplasmic Ca^{2+} release from the ER and triggers SOCE in endothelial cells [56-58]. Thrombin is a pro-inflammatory agonist that has been

shown to activate microglia via G protein-coupled proteinase-activated receptors (PARs) [59]. We demonstrated that loss of RGS10 in BV2 microglia enhanced thrombin-mediated expression of pro-inflammatory genes including COX-2, TNFα, and IL-6, indicating that RGS10's anti-inflammatory effect is not limited to the regulation of TLR4 response. Inhibition of SOCE also blunted the upregulation of thrombin-stimulated expression of these pro-inflammatory genes in response to RGS10 loss. Therefore, the ability of RGS10 to regulate both thrombin and LPS pro-inflammatory responses through a common downstream mechanism involving SOCE suggests a broad anti-inflammatory role for RGS10. We have previously demonstrated that RGS10 does not regulate acute activation of NFkB, MAPK, and AKT pathways following LPS stimulation [4].NFAT is a likely candidate for mediating the effect of RGS10 downstream of Orai-calcineurin activation, and multiple NFAT family members; in particular NFATc1 and NFATc2 have been reported to have prominent expression in microglia[60]. Ongoing studies will characterize the effect of RGS10 on NFAT expression, activation, and translocation in response to multiple stimuli.

STIM1 and STIM2 are localized throughout the ER under basal conditions with high ER calcium, but upon ER calcium depletion, the STIM proteins undergo conformational rearrangement and form homo- and/or hetero-dimers that translocate to ER-PM junctions, where they can bind and activate Orai channels, triggering SOCE [61, 62]. Despite the close homology between STIM1 and STIM2, our results indicate that RGS10 specifically interacts with STIM2 and not STIM1, and the interaction with STIM2 does not depend on calcium. These results are consistent with a basal interaction of RGS10 and STIM2 that does not include STIM1-STIM2 heterodimers. It is possible that RGS10 interaction with STIM2 may inhibit the formation of STIM1/2 heterodimers, which would allow RGS10 to indirectly impact STIM1 function without physically interacting with STIM1. While this study uncovered a functional link between RGS10 and STIM2, it did not delineate the specific role of this biochemical interaction. It is plausible that the anti-inflammatory function of RGS10 and its ability to alter SOCE may be mediated by its interaction with STIM2, which may alter the functional response of STIM2 including conformational activation, dimerization, and/or STIM/Orai coupling [61, 62]. Ongoing biochemical and signaling studies are examining the role and biochemical requirements of the RGS10-STIM2 interaction. For example, it is important to determine if STIM2 directly binds RGS10 or if their interaction reflects mutual enrichment in a multi-protein complex regulated by other factors such as subcellular localization, G protein activation, or additional binding partners. Given the lack of defined functional domains in RGS10 other than the highly conserved RGS domain, which is shared among all members of the RGS protein family [63], further biochemical studies should determine if the RGS10-STIM2 interaction is mediated by the RGS domain and whether STIM2 also associates with this domain in other RGS proteins.

Calcium Release-Activated Calcium (CRAC) proteins including Orai channels represent the primary route for store-operated calcium entry (SOCE). Despite limited knowledge of the role of microglial SOCE, STIM2 and the components of CRAC channels have been implicated in several acute and chronic neuropathological conditions including PD, AD, ischemic stroke, and traumatic brain injury (TBI) [64]. Therefore, RGS10's ability to suppress SOCE and its broad anti-inflammatory response in microglia has implications for many neurodegenerative diseases with underlying chronic neuroinflammation. RGS10 is

also expressed in multiple other cells and modulates immune signaling and other functions in macrophages [65], osteoclasts [23, 66], T-lymphocytes [45, 67], cardiomyocytes [46], neurons [5], and cancer cells [41, 44]. Although many functions of RGS10 have been identified in these systems, the exact molecular mechanisms governing these functions are not understood. Therefore, the involvement of STIM2 and SOCE in RGS10's anti-inflammatory molecular mechanism has implications beyond neuroinflammation, to include diverse pathologies in which RGS10 function is implicated, such as multiple sclerosis [45], cancer chemoresistance [41, 44], cardiac hypertrophy [46], and bone disorders [23, 66].

4. Conclusion

This study identified a novel interaction between RGS10 and STIM2 in microglia and demonstrated that STIM2 and the downstream SOCE pathway are essential for LPS-induced inflammatory gene expression. Suppression of STIM2 expression or inhibition of the Orai-calcineurin signaling axis impaired RGS10's inhibition of inflammatory gene expression. Our study also revealed a new role for RGS10 in regulating SOCE, which may account for the G protein-independent anti-inflammatory mechanism of RGS10 in microglia.

5. Materials and Methods

5.1. Cells and Reagents

The murine BV2 microglial cell line was a generous gift from G. Hasko at the University of Medicine and Dentistry of New Jersey (Newark, NJ), and was generated by Blasi et al. [68]. RAW 264.7 macrophage cell line was purchased from ATCC (T1B-71). The N9 microglia cell line was a generous gift from N. Filipov at the University of Georgia [69]. CRISPR/Cas9 control and Crispr/Cas9 RGS10 knockout BV2 cell lines were established by our group, as previously described [4]. Wild type and RGS10 knockout breeder mice were gifted to us from J.K Lee at the University of Georgia, and have previously been used for neuroinflammation research[5-7]. The compounds used in this study are Lipopolysaccharide (Sigma-Aldrich: L2880), Thrombin (Sigma-Aldrich: T4648), Cyclosporin A (FagronLab: 803651), YM-58483 (Tocris Bioscience: 3939), and Thapsigargin (Abcam: ab120286).

5.2. Cell Culture

BV2, N9, and RAW264.7 cell lines and isolated mouse peritoneal macrophages were maintained in Dulbecco's modified Eagle's medium (DMEM) (37 °C, 5% CO_2) supplemented with 10% low-endotoxin fetal bovine serum (FBS) (Thermo Fischer Scientific: 10082147), and 1% penicillin/streptomycin (P/S). Mixed glia and isolated microglia cultures were maintained similarly but using DMEM/Hams F-12 50/50 mix medium (Corning: 10-090-CV).

5.3. Primary Cell Isolation

Primary microglia were isolated from mixed cortical cultures using a modified protocol adapted from previous studies[70, 71]. Briefly, 1-3 days old wild type and RGS10 knockout postnatal mouse pups were anesthetized using isoflurane, and whole brains were collected. After removing the cerebellum and meninges, tissues from the two hemispheres were cut

into small pieces and digested with 0.25% trypsin for 20 min at 37°C. Digested tissue was further mechanically dissociated by trituration and filtered through a 40 μm filter. Single-cell suspensions were plated onto a poly-D-lysine (PDL)-coated T75 tissue culture flasks (2-3 brains/flask) and maintained in FBS-containing DMEM/F12 medium. The growth medium was changed on days 3 and 7, and an additional medium was added to the mixed glia culture on day 10 followed by microglia isolation on day 15. Microglia were isolated by shaking the confluent mixed glial culture at 130 RPM (37°C) for 3-4h, and non-adherent microglia cells were centrifuged for 5 min at 400g (4°C) and resuspended with growth media. Cells were plated in PDL-coated 12-well plates (0.25×10^6 cells/well) and cultured for additional 2 days prior to experimental treatments.

Mouse peritoneal macrophages were elicited by intraperitoneal injection of 3% thioglycolate broth from adult mice (Millipore Sigma: 70157). Macrophages were harvested 4 days post-injection via peritoneal lavage with cold PBS, as previously detailed[72]. Harvested cells were cultured for 24h in a 10cm dish with DMEM, supplemented with 10% FBS and 1% P/S. After 24h, cells washed with PBS and continued to grow for an additional 24h prior to immunoprecipitation experiments.

5.4. Immunoprecipitation

Immunoprecipitation (IP) experiments for mass spectrometry (MS) analysis were performed using BV2 microglia cells plated in six 15 cm dishes and grown to ~85% confluency. Cells were washed twice with PBS and harvested with 1mL of modified lysis buffer (50 mM Tris HCl, 150 mM NaCl, 6mM $MgCl_2$, 1% Nonidet P-40, 0.5% sodium deoxycholate), containing protease/phosphatase inhibitor cocktail (Cell Signaling Technology). Cell lysates were incubated on ice for 30 min, and insoluble cellular debris was removed by centrifugation at 27,216 g for 10 min at 4°C. Cleared lysates were incubated overnight at 4°C with 2 μg/mL agarose-conjugated goat polyclonal RGS10 antibody (Santa Cruz Biotechnology: sc-6206AC) or agarose-conjugated goat IgG antibody (Santa Cruz Biotechnology: sc-2346). Samples were centrifuged at 410 g for 5 min, and pellets were washed 3 times with wash buffer (50mM Tris HCl, 150 mM NaCl, 6 mM $MgCl_2$). Immunoprecipitating proteins were eluted from agarose-conjugated beads by incubation with 100 μL elution buffer (0.15 M glycine, pH 2.6) for 10 min at room temperature with gentle shaking. Eluted samples were centrifuged again to remove beads (410g, 5 min, 4°C), and the supernatant was neutralized with an equal volume of 1M Tris HCl, pH 8, and subsequently subjected to overnight acetone precipitation (4x volume) at −20° C. Samples were centrifuged twice (16,000 g, 10 min, 4°C) with an acetone wash in between centrifugation. The final pellet was air-dried for 30 min prior to LC/MS-MS analysis.

Follow-up co-IP validations were performed in cells grown in a 10cm dish. Cells were harvested as indicated above, but lysates were split in half and immunoprecipitated with either 2 μg/mL of goat RGS10 antibody (Santa Cruz Biotechnology: sc-6206) or normal goat IgG (R&D Systems: AB-109-C). Subsequently, lysates were incubated with 20 μL of a 50% slurry of Protein G-conjugated sepharose (GE Healthcare: 17-0618-01) for 2 h at 4°C, and centrifuged at 410 g for 5 minutes. The beads were washed twice with PBS and resuspended with 50 μl of 2X SDS-PAGE sample buffer for western blot analysis. Co-IP

experiments in N9 cells, RAW264.7 cells, and primary peritoneal macrophages were conducted following the same protocol. Calcium-containing co-IP experiments were conducted similarly, but cleared lysates were incubated with either $CaCl_2$ (1mM) or EGTA (0.5 mM) for 1 h at 4°C prior to immunoprecipitation.

5.5. Mass Spectrometry

Acetone precipitated immunoprecipitates were resuspended in digestion buffer (100 mM Tris pH 8.5, 8M urea) and then reduced, alkylated, and digested by the sequential addition of lys-c and trypsin proteases as previously described[73]. Digested samples were then fractioned online by C18 reversed-phase chromatography and then analyzed by tandem mass spectrometry using a Thermofisher Fusion Lumos Mass Spectrometer as described[74]. MS/MS data were analyzed using MSGF+ for peptide identification, Percolator for decoy database-based statistical filtering, Fido for protein interference, and SAINT algorithm for the identification of proteins enriched in RGS10 IPs relative to control IPs[75-77].

5.1. Quantitative Real-Time Polymerase Chain Reaction

Total RNA was isolated from cells with TRIzol reagent (Invitrogen). cDNA was synthesized using the High-Capacity Reverse Transcriptase cDNA kit (Applied Biosystems). Real-time PCR was performed using SYBR Green PCR Master Mix (Applied Biosystems). The housekeeping β-actin gene was used for data normalization and relative mRNA abundance was calculated using the $2^{-\Delta\Delta CT}$ method. Mouse primers sequences used for RT-PCR are listed as follows: RGS10, 5'-CCCGGAGAATCTTCTGGAAGACC-3' (forward) and 5'-CTGCTTCCTGTCCTCCGTTTTC-3' (reverse); TNFα, 5'-CCTGTAGCCCACGTCGTAG-3' (forward) and GGGAGTAGACAAGGTACAACCC (reverse); COX-2, 5'-TGCAAGATCCACAGCCTACC-3' (forward) and 5'-GCTCAGTTGAACGCCTTTTG-3' (reverse); IL-6, 5'-CTGCAAGAGACTTCCATCCAG-'3 (forward) and 5'-AGTGGTATAGACAGGTCTGTTGG-3' (reverse); β-actin, 5'-GGCTGTATTCCCCTCCATCG-3' (forward) and 5'-CCAGTTGGTAACAATGCCATGT-3' (reverse). Primers for RGS10 and TNFα were purchased from Integrated DNA Technology, and COX-2 and β-actin primers were obtained from Sigma-Aldrich.

5.2. Western Blot Analysis

Cell lysates were subject to SDS-PAGE followed by transfer to nitrocellulose membranes using standard protocols, as previously detailed[9]. Membranes were blocked with 5% milk and incubated overnight with the following primary antibodies: goat anti-RGS10 (Santa Cruz Biotechnology: sc-6206), mouse anti-COX-2 (Santa Cruz Biotechnology: sc-166475), mouse anti-Syntaxin 5 (Santa Cruz Biotechnology: sc-365124), mouse anti-GAPDH (Thermo Fisher Scientific: am4300), mouse anti-Calmodulin (MilliporeSigma: 05-173), rabbit anti-GNAI3 (Proteintech: 11641-1-AP), rabbit anti-STIM1 (Proteintech: 11565-1-AP), rabbit anti-STIM2 (Proteintech: 21192-1-AP), and rabbit anti-PDE4A (Proteintech: 16226-1-AP). Primary antibodies, except for GAPDH (1:6000), were used at 1:500-1:1000 dilutions. Membranes were subsequently incubated for 1h with the following secondary antibodies (1:5000): donkey anti-goat IgG-HRP (Santa Cruz Biotechnology: sc-2020), goat anti-rabbit IgG-HRP (MilliporeSigma: 12-348), and goat anti-mouse IgG HRP (Bethyl

Laboratories: A90-116P). Immunoreactivity of HRP was detected using Supersignal West Pico Chemiluminescent Substrate (Pierce). Western Blot images were quantified using FluorChem HD2 software (Proteinsimple), and quantified data were normalized to the endogenous control GAPDH.

5.3. Small Interfering RNA Transfection

Mouse STIM2 small interfering RNA (siRNA) (sc-76592) and control siRNA (sc-37007) were purchased from Santa Cruz Biotechnology. Transfection was performed using Lipofectamine-LTX with PLUS reagent (Thermo Fisher Scientific: 15338100) according to the manufacturer's protocol, with a final siRNA concentration of 60 nM in an antibiotic-free culture media. Cells were harvested 48 h after transfection. STIM2 protein western blotting was used to assess knockdown efficiency, and STIM1 protein level was measured to assess target specificity.

5.4. Calcium Imaging

CRISPR-control BV2 and CRISPR-RGS10 knockout cells were plated on 35mm MatTek glass-bottom dishes. Prior to loading, cells were washed twice with Ringer Solution (155 mM NaCl, 3 mM KCl, 1.8 mM $CaCl_2$, 1 mM $MgCl_2$, 3 mM NaH_2PO_4, 10 mM Hepes, pH 7.3, and glucose 10 mM). Cells were loaded with 5μM Cal-520, AM (Abcam: ab171868) in Ringer buffer in the presence of 1mM Probenecid (Sigma Aldrich: P8761) in the dark at 37°C for 20 mins. Cells were washed twice and the media was replaced with Ringer Buffer supplemented with 100 μM EGTA to chelate contaminating calcium. Fluorescent imaging was performed at 37°C using an Olympus 1X-71 inverted fluorescence microscope with a Photometrics CoolSnapHQ charge-coupled device (CCD) camera driven by DeltaVision software (Applied Precision). Images were collected every 3 s for a total of 15 min, and traces were transformed in videos using SoftWorx suite 2.0 software (Applied Precision). Images were processed using the FIJI ImageJ software suite[78], and the fluorescence signal at each time point was normalized to the baseline fluorescence of each cell.

5.5. Statistical Analysis

All quantified data were analyzed using GraphPad Prism Software and assessed for normality using D'Agostino & Pearson omnibus normality test. Statistical differences between groups were determined using student's t-test or one-way ANOVA followed by Tukey post hoc analysis. Data are presented as mean ± SEM pooled from a minimum of three independent experiments. The p-value cutoff ranges are indicated by *$p < 0.05$, **$p<0.01$, and ***$p<0.001$.

Supplementary Material

Refer to Web version on PubMed Central for supplementary material.

Acknowledgements

The content is solely the responsibility of the authors and does not necessarily represent the official views of the National Institutes of Health.

Funding

GM089778 to J.A.W., NS101161 and NS109303 to S.B.H., AI128356 to S.M., T32AI060546 to S.A.V.

References

[1]. Furman D, Campisi J, Verdin E, Carrera-Bastos P, Targ S, Franceschi C, Ferrucci L, Gilroy DW, Fasano A, Miller GW, Miller AH, Mantovani A, Weyand CM, Barzilai N, Goronzy JJ, Rando TA, Effros RB, Lucia A, Kleinstreuer N, Slavich GM, Chronic inflammation in the etiology of disease across the life span, Nat Med 25(12) (2019) 1822–1832. [PubMed: 31806905]

[2]. Hickman S, Izzy S, Sen P, Morsett L, El Khoury J, Microglia in neurodegeneration, Nat Neurosci 21(10) (2018)1359–1369. [PubMed: 30258234]

[3]. Lull ME, Block ML, Microglial activation and chronic neurodegeneration, Neurotherapeutics 7(4) (2010) 354–65. [PubMed: 20880500]

[4]. Alqinyah M, Almutairi F, Wendimu MY, Hooks SB, RGS10 Regulates the Expression of Cyclooxygenase-2 and Tumor Necrosis Factor Alpha through a G Protein-Independent Mechanism, Mol Pharmacol 94(4) (2018) 1103–1113. [PubMed: 30049816]

[5]. Lee JK, Chung J, Druey KM, Tansey MG, RGS10 exerts a neuroprotective role through the PKA/c-AMP response-element (CREB) pathway in dopaminergic neuron-like cells, J Neurochem 122(2) (2012) 333–43. [PubMed: 22564151]

[6]. Lee JK, Chung J, McAlpine FE, Tansey MG, Regulator of G-protein signaling-10 negatively regulates NF-kappaB in microglia and neuroprotects dopaminergic neurons in hemiparkinsonian rats, J Neurosci 31(33) (2011) 11879–88. [PubMed: 21849548]

[7]. Lee JK, McCoy MK, Harms AS, Ruhn KA, Gold SJ, Tansey MG, Regulator of G-protein signaling 10 promotes dopaminergic neuron survival via regulation of the microglial inflammatory response, J Neurosci 28(34) (2008) 8517–28. [PubMed: 18716210]

[8]. Henn A, Lund S, Hedtjarn M, Schrattenholz A, Porzgen P, Leist M, The suitability of BV2 cells as alternative model system for primary microglia cultures or for animal experiments examining brain inflammation, ALTEX 26(2) (2009) 83–94. [PubMed: 19565166]

[9]. Alqinyah M, Maganti N, Ali MW, Yadav R, Gao M, Cacan E, Weng HR, Greer SF, Hooks SB, Regulator of G Protein Signaling 10 (Rgs10) Expression Is Transcriptionally Silenced in Activated Microglia by Histone Deacetylase Activity, Mol Pharmacol 91(3) (2017) 197–207. [PubMed: 28031332]

[10]. Popov S, Yu K, Kozasa T, Wilkie TM, The regulators of G protein signaling (RGS) domains of RGS4, RGS10, and GAIP retain GTPase activating protein activity in vitro, Proc Natl Acad Sci U S A 94(14) (1997) 7216–20. [PubMed: 9207071]

[11]. Watson N, Linder ME, Druey KM, Kehrl JH, Blumer KJ, RGS family members: GTPase-activating proteins for heterotrimeric G-protein alpha-subunits, Nature 383(6596) (1996) 172–5. [PubMed: 8774882]

[12]. Berna-Erro A, Jardin I, Salido GM, Rosado JA, Role of STIM2 in cell function and physiopathology, J Physiol 595(10) (2017) 3111–3128. [PubMed: 28087881]

[13]. Hoth M, Niemeyer BA, The neglected CRAC proteins: Orai2, Orai3, and STIM2, Current topics in membranes, Elsevier2013, pp. 237–271.

[14]. Ong HL, de Souza LB, Zheng C, Cheng KT, Liu X, Goldsmith CM, Feske S, Ambudkar IS, STIM2 enhances receptor-stimulated Ca(2)(+) signaling by promoting recruitment of STIM1 to the endoplasmic reticulum-plasma membrane junctions, Sci Signal 8(359) (2015) ra3. [PubMed: 25587190]

[15]. Chatterjee TK, Fisher RA, Cytoplasmic, nuclear, and golgi localization of RGS proteins. Evidence for N-terminal and RGS domain sequences as intracellular targeting motifs, J Biol Chem 275(31) (2000) 24013–21. [PubMed: 10791963]

[16]. Chang WC, Store-operated calcium channels and pro-inflammatory signals, Acta Pharmacol Sin 27(7) (2006) 813–20. [PubMed: 16787563]

[17]. Michaelis M, Nieswandt B, Stegner D, Eilers J, Kraft R, STIM1, STIM2, and Orai1 regulate store-operated calcium entry and purinergic activation of microglia, Glia 63(4) (2015) 652–63. [PubMed: 25471906]

[18]. Sogkas G, Stegner D, Syed SN, Vogtle T, Rau E, Gewecke B, Schmidt RE, Nieswandt B, Gessner JE, Cooperative and alternate functions for STIM1 and STIM2 in macrophage activation and in the context of inflammation, Immun Inflamm Dis 3(3) (2015) 154–70. [PubMed: 26417434]

[19]. Williams RT, Manji SS, Parker NJ, Hancock MS, Van Stekelenburg L, Eid JP, Senior PV, Kazenwadel JS, Shandala T, Saint R, Smith PJ, Dziadek MA, Identification and characterization of the STIM (stromal interaction molecule) gene family: coding for a novel class of transmembrane proteins, Biochem J 357(Pt 3) (2001) 673–85. [PubMed: 11463338]

[20]. Kraft R, STIM and ORAI proteins in the nervous system, Channels (Austin) 9(5) (2015) 245–52. [PubMed: 26218135]

[21]. Bauer MC, O'Connell D, Cahill DJ, Linse S, Calmodulin binding to the polybasic C-termini of STIM proteins involved in store-operated calcium entry, Biochemistry 47(23) (2008) 6089–91. [PubMed: 18484746]

[22]. Popov SG, Krishna UM, Falck JR, Wilkie TM, Ca2+/Calmodulin reverses phosphatidylinositol 3,4, 5-trisphosphate-dependent inhibition of regulators of G protein-signaling GTPase-activating protein activity, J Biol Chem 275(25) (2000) 18962–8. [PubMed: 10747990]

[23]. Yang S, Li YP, RGS10-null mutation impairs osteoclast differentiation resulting from the loss of [Ca2+]i oscillation regulation, Genes Dev 21(14) (2007) 1803–16. [PubMed: 17626792]

[24]. Kang YJ, Wingerd BA, Arakawa T, Smith WL, Cyclooxygenase-2 gene transcription in a macrophage model of inflammation, J Immunol 177(11) (2006) 8111–22. [PubMed: 17114486]

[25]. Rex J, Albrecht U, Ehlting C, Thomas M, Zanger UM, Sawodny O, Haussinger D, Ederer M, Feuer R, Bode JG, Model-Based Characterization of Inflammatory Gene Expression Patterns of Activated Macrophages, PLoS Comput Biol 12(7) (2016) e1005018. [PubMed: 27464342]

[26]. Yoshikawa S, Oh-Hora M, Hashimoto R, Nagao T, Peters L, Egawa M, Ohta T, Miyake K, Adachi T, Kawano Y, Yamanishi Y, Karasuyama H, Pivotal role of STIM2, but not STIM1, in IL-4 production by IL-3-stimulated murine basophils, Sci Signal 12(576) (2019).

[27]. Font-Nieves M, Sans-Fons MG, Gorina R, Bonfill-Teixidor E, Salas-Perdomo A, Marquez-Kisinousky L, Santalucia T, Planas AM, Induction of COX-2 enzyme and down-regulation of COX-1 expression by lipopolysaccharide (LPS) control prostaglandin E2 production in astrocytes, J Biol Chem 287(9) (2012) 6454–68. [PubMed: 22219191]

[28]. Ikeda-Matsuo Y, Ikegaya Y, Matsuki N, Uematsu S, Akira S, Sasaki Y, Microglia-specific expression of microsomal prostaglandin E2 synthase-1 contributes to lipopolysaccharide-induced prostaglandin E2 production, J Neurochem 94(6) (2005) 1546–58. [PubMed: 16000148]

[29]. Nelson HA, Leech CA, Kopp RF, Roe MW, Interplay between ER Ca(2+) Binding Proteins, STIM1 and STIM2, Is Required for Store-Operated Ca(2+) Entry, Int J Mol Sci 19(5) (2018).

[30]. Soboloff J, Rothberg BS, Madesh M, Gill DL, STIM proteins: dynamic calcium signal transducers, Nat Rev Mol Cell Biol 13(9) (2012) 549–65. [PubMed: 22914293]

[31]. Hogan PG, Lewis RS, Rao A, Molecular basis of calcium signaling in lymphocytes: STIM and ORAI, Annu Rev Immunol 28 (2010) 491–533. [PubMed: 20307213]

[32]. Kar P, Parekh A, STIM proteins, Orai1 and gene expression, Channels (Austin) 7(5) (2013) 374–8. [PubMed: 23765192]

[33]. Park YJ, Yoo SA, Kim M, Kim WU, The Role of Calcium-Calcineurin-NFAT Signaling Pathway in Health and Autoimmune Diseases, Front Immunol 11 (2020) 195. [PubMed: 32210952]

[34]. Hogan PG, Rao A, Store-operated calcium entry: Mechanisms and modulation, Biochem Biophys Res Commun 460(1) (2015) 40–9. [PubMed: 25998732]

[35]. Batista CRA, Gomes GF, Candelario-Jalil E, Fiebich BL, de Oliveira ACP, Lipopolysaccharide-Induced Neuroinflammation as a Bridge to Understand Neurodegeneration, Int J Mol Sci 20(9) (2019).

[36]. Lively S, Schlichter LC, Microglia Responses to Pro-inflammatory Stimuli (LPS, IFNgamma +TNFalpha) and Reprogramming by Resolving Cytokines (IL-4, IL-10), Front Cell Neurosci 12 (2018) 215. [PubMed: 30087595]

[37]. Krenzlin H, Lorenz V, Danckwardt S, Kempski O, Alessandri B, The Importance of Thrombin in Cerebral Injury and Disease, Int J Mol Sci 17(1) (2016).

[38]. Subramaniam SR, Federoff HJ, Targeting Microglial Activation States as a Therapeutic Avenue in Parkinson's Disease, Front Aging Neurosci 9 (2017) 176. [PubMed: 28642697]

[39]. Fatoba O, Itokazu T, Yamashita T, Microglia as therapeutic target in central nervous system disorders, J Pharmacol Sci 144(3) (2020) 102–118. [PubMed: 32921391]

[40]. Almutairi F, Lee JK, Rada B, Regulator of G protein signaling 10: Structure, expression and functions in cellular physiology and diseases, Cell Signal 75 (2020) 109765. [PubMed: 32882407]

[41]. Ali MW, Cacan E, Liu Y, Pierce JY, Creasman WT, Murph MM, Govindarajan R, Eblen ST, Greer SF, Hooks SB, Transcriptional suppression, DNA methylation, and histone deacetylation of the regulator of G-protein signaling 10 (RGS10) gene in ovarian cancer cells, PloS one 8(3) (2013) e60185. [PubMed: 23533674]

[42]. Alqinyah M, Almutairi F, Wendimu MY, Hooks SB, RGS10 Regulates the Expression of Cyclooxygenase-2 and Tumor Necrosis Factor Alpha through a G Protein–Independent Mechanism, Molecular pharmacology 94(4) (2018) 1103–1113. [PubMed: 30049816]

[43]. Hooks SB, Callihan P, Altman MK, Hurst JH, Ali MW, Murph MM, Regulators of G-Protein signaling RGS10 and RGS17 regulate chemoresistance in ovarian cancer cells, Mol Cancer 9 (2010) 289. [PubMed: 21044322]

[44]. Hooks SB, Murph MM, Cellular deficiency in the RGS10 protein facilitates chemoresistant ovarian cancer, Future Med Chem 7(12) (2015) 1483–9. [PubMed: 26293348]

[45]. Lee JK, Kannarkat GT, Chung J, Joon Lee H, Graham KL, Tansey MG, RGS10 deficiency ameliorates the severity of disease in experimental autoimmune encephalomyelitis, J Neuroinflammation 13 (2016) 24. [PubMed: 26831924]

[46]. Miao R, Lu Y, Xing X, Li Y, Huang Z, Zhong H, Huang Y, Chen AF, Tang X, Li H, Cai J, Yuan H, Regulator of G-Protein Signaling 10 Negatively Regulates Cardiac Remodeling by Blocking Mitogen-Activated Protein Kinase-Extracellular Signal-Regulated Protein Kinase 1/2 Signaling, Hypertension 67(1) (2016) 86–98. [PubMed: 26573707]

[47]. Ong HL, de Souza LB, Zheng C, Cheng KT, Liu X, Goldsmith CM, Feske S, Ambudkar IS, STIM2 enhances receptor-stimulated Ca^{2+} signaling by promoting recruitment of STIM1 to the endoplasmic reticulum–plasma membrane junctions, Science Signaling 8(359) (2015) ra3–ra3. [PubMed: 25587190]

[48]. Akundi RS, Candelario-Jalil E, Hess S, Hull M, Lieb K, Gebicke-Haerter PJ, Fiebich BL, Signal transduction pathways regulating cyclooxygenase-2 in lipopolysaccharide-activated primary rat microglia, Glia 51(3) (2005) 199–208. [PubMed: 15800925]

[49]. Chun KS, Surh YJ, Signal transduction pathways regulating cyclooxygenase-2 expression: potential molecular targets for chemoprevention, Biochem Pharmacol 68(6) (2004) 1089–100. [PubMed: 15313405]

[50]. Eliopoulos AG, Dumitru CD, Wang CC, Cho J, Tsichlis PN, Induction of COX-2 by LPS in macrophages is regulated by Tpl2-dependent CREB activation signals, EMBO J 21(18) (2002) 4831–40. [PubMed: 12234923]

[51]. Klein T, Shephard P, Kleinert H, Komhoff M, Regulation of cyclooxygenase-2 expression by cyclic AMP, Biochim Biophys Acta 1773(11) (2007) 1605–18. [PubMed: 17945363]

[52]. McElroy SJ, Hobbs S, Kallen M, Tejera N, Rosen MJ, Grishin A, Matta P, Schneider C, Upperman J, Ford H, Polk DB, Weitkamp JH, Transactivation of EGFR by LPS induces COX-2 expression in enterocytes, PloS one 7(5) (2012) e38373. [PubMed: 22675459]

[53]. Wong JH, Ho KH, Nam S, Hsu WL, Lin CH, Chang CM, Wang JY, Chang WC, Store-operated Ca(2+) Entry Facilitates the Lipopolysaccharide-induced Cyclooxygenase-2 Expression in Gastric Cancer Cells, Sci Rep 7(1) (2017) 12813. [PubMed: 29038542]

[54]. Mizuma A, Kim JY, Kacimi R, Stauderman K, Dunn M, Hebbar S, Yenari MA, Microglial Calcium Release-Activated Calcium Channel Inhibition Improves Outcome from Experimental Traumatic Brain Injury and Microglia-Induced Neuronal Death, J Neurotrauma 36(7) (2019) 996–1007. [PubMed: 30351197]

[55]. Newton K, Dixit VM, Signaling in innate immunity and inflammation, Cold Spring Harb Perspect Biol 4(3) (2012).

[56]. Spinelli AM, Trebak M, Orai channel-mediated Ca2+ signals in vascular and airway smooth muscle, Am J Physiol Cell Physiol 310(6) (2016) C402–13. [PubMed: 26718630]

[57]. Stolwijk JA, Zhang X, Gueguinou M, Zhang W, Matrougui K, Renken C, Trebak M, Calcium Signaling Is Dispensable for Receptor Regulation of Endothelial Barrier Function, J Biol Chem 291(44) (2016) 22894–22912. [PubMed: 27624938]

[58]. Sundivakkam PC, Natarajan V, Malik AB, Tiruppathi C, Store-operated Ca2+ entry (SOCE) induced by protease-activated receptor-1 mediates STIM1 protein phosphorylation to inhibit SOCE in endothelial cells through AMP-activated protein kinase and p38beta mitogen-activated protein kinase, J Biol Chem 288(23) (2013) 17030–41. [PubMed: 23625915]

[59]. Hanisch UK, van Rossum D, Xie Y, Gast K, Misselwitz R, Auriola S, Goldsteins G, Koistinaho J, Kettenmann H, Moller T, The microglia-activating potential of thrombin: the protease is not involved in the induction of proinflammatory cytokines and chemokines, J Biol Chem 279(50) (2004) 51880–7. [PubMed: 15452111]

[60]. Nagamoto-Combs K, Combs CK, Microglial phenotype is regulated by activity of the transcription factor, NFAT (nuclear factor of activated T cells), J Neurosci 30(28) (2010) 9641–6. [PubMed: 20631193]

[61]. Palty R, Fu Z, Isacoff EY, Sequential Steps of CRAC Channel Activation, Cell Rep 19(9) (2017) 1929–1939. [PubMed: 28564609]

[62]. Stathopulos PB, Zheng L, Ikura M, Stromal interaction molecule (STIM) 1 and STIM2 calcium sensing regions exhibit distinct unfolding and oligomerization kinetics, J Biol Chem 284(2) (2009) 728–32. [PubMed: 19019825]

[63]. Hollinger S, Hepler JR, Cellular regulation of RGS proteins: modulators and integrators of G protein signaling, Pharmacological reviews 54(3) (2002) 527–59. [PubMed: 12223533]

[64]. Secondo A, Bagetta G, Amantea D, On the role of store-operated calcium entry in acute and chronic neurodegenerative diseases, Frontiers in molecular neuroscience 11 (2018) 87. [PubMed: 29623030]

[65]. Lee JK, Chung J, Kannarkat GT, Tansey MG, Critical Role of Regulator G-Protein Signaling 10 (RGS10) in Modulating Macrophage M1/M2 Activation, PloS one 8(11) (2013) e81785. [PubMed: 24278459]

[66]. Yang S, Hao L, McConnell M, Zhou X, Wang M, Zhang Y, Mountz JD, Reddy M, Eleazer PD, Li YP, Chen W, Inhibition of Rgs10 Expression Prevents Immune Cell Infiltration in Bacteria-induced Inflammatory Lesions and Osteoclast-mediated Bone Destruction, Bone Res 1(3) (2013) 267–281. [PubMed: 24761229]

[67]. Garcia-Bernal D, Dios-Esponera A, Sotillo-Mallo E, Garcia-Verdugo R, Arellano-Sanchez N, Teixido J, RGS10 restricts upregulation by chemokines of T cell adhesion mediated by alpha4beta1 and alphaLbeta2 integrins, J Immunol 187(3) (2011) 1264–72. [PubMed: 21705617]

[68]. Blasi E, Barluzzi R, Bocchini V, Mazzolla R, Bistoni F, Immortalization of murine microglial cells by a v-raf/v-myc carrying retrovirus, J Neuroimmunol 27(2-3) (1990) 229–37. [PubMed: 2110186]

[69]. Crittenden P, Filipov N, Manganese-induced potentiation of in vitro proinflammatory cytokine production by activated microglial cells is associated with persistent activation of p38 MAPK, Toxicology in Vitro 22(1) (2008) 18–27. [PubMed: 17845838]

[70]. Lian H, Roy E, Zheng H, Protocol for Primary Microglial Culture Preparation, Bio Protoc 6(21) (2016).

[71]. Yao Y, Tsirka SE, The C terminus of mouse monocyte chemoattractant protein 1 (MCP1) mediates MCP1 dimerization while blocking its chemotactic potency, J Biol Chem 285(41) (2010) 31509–16. [PubMed: 20682771]

[72]. Zhang X, Goncalves R, Mosser DM, The isolation and characterization of murine macrophages, Curr Protoc Immunol Chapter 14 (2008) Unit 14 1.

[73]. Wohlschlegel JA, Identification of SUMO-conjugated proteins and their SUMO attachment sites using proteomic mass spectrometry, Methods Mol Biol 497 (2009) 33–49. [PubMed: 19107409]

[74]. Stehling O, Vashisht AA, Mascarenhas J, Jonsson ZO, Sharma T, Netz DJ, Pierik AJ, Wohlschlegel JA, Lill R, MMS19 assembles iron-sulfur proteins required for DNA metabolism and genomic integrity, Science 337(6091) (2012) 195–9. [PubMed: 22678362]

[75]. Choi H, Liu G, Mellacheruvu D, Tyers M, Gingras AC, Nesvizhskii AI, Analyzing protein-protein interactions from affinity purification-mass spectrometry data with SAINT, Curr Protoc Bioinformatics Chapter 8 (2012) Unit8 15.

[76]. Granholm V, Kim S, Navarro JC, Sjolund E, Smith RD, Kall L, Fast and accurate database searches with MS-GF+Percolator, J Proteome Res 13(2) (2014) 890–7. [PubMed: 24344789]

[77]. Serang O, Noble WS, Faster mass spectrometry-based protein inference: junction trees are more efficient than sampling and marginalization by enumeration, IEEE/ACM Trans Comput Biol Bioinform 9(3) (2012) 809–17. [PubMed: 22331862]

[78]. Schindelin J, Arganda-Carreras I, Frise E, Kaynig V, Longair M, Pietzsch T, Preibisch S, Rueden C, Saalfeld S, Schmid B, Tinevez JY, White DJ, Hartenstein V, Eliceiri K, Tomancak P, Cardona A, Fiji: an open-source platform for biological-image analysis, Nat Methods 9(7) (2012) 676–82. [PubMed: 22743772]

- RGS10 has diverse non-canonical interaction partners in microglia, including the regulator of store operated calcium entry STIM2.
- RGS10 downregulates Thrombin- and LPS-induced inflammatory gene expression via STIM2 and downstream SOCE pathway.
- RGS10 blunts SOCE triggered by store calcium depletion in microglia.

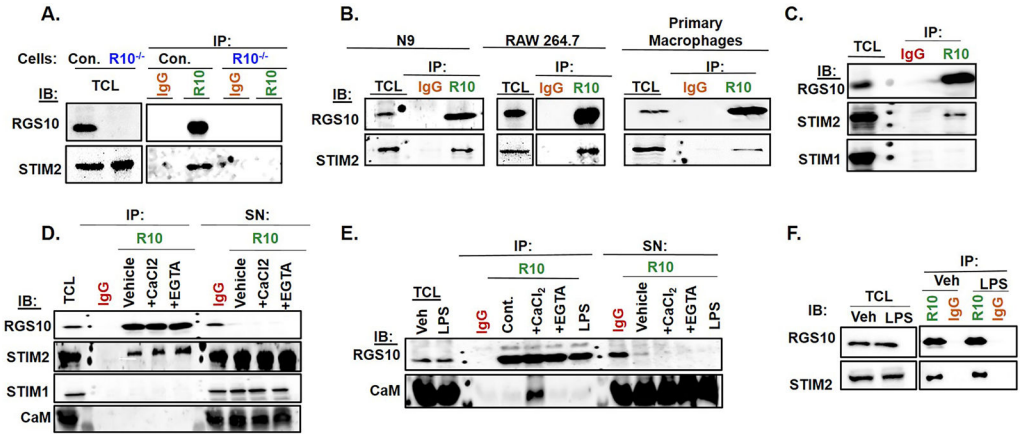

Figure 1. Specificity and regulation of RGS10-STIM2 interaction.

A) Control (Con.) and RGS10 knockout ($R10^{-/-}$) BV2 total cell lysate (TCL) immunoprecipitated (IP) with RGS10 (R10) and control (IgG) antibodies followed by immunoblotting (IB) for RGS10 and STIM2. **B)** RGS10 IP in N9 microglia (left panel), RAW264.7 macrophages (middle panel), and primary peritoneal macrophages (right panel), followed by IB for RGS10 and STIM2. **C)** RGS10 IP in wild type BV2 cells followed by IB for RGS10, STIM2, and STIM1. **D.** RGS10 and control IP from BV2 cells incubated for 1 hour with lysis buffer alone (Veh) or in the presence of either $CaCl_2$ (1mM) or EGTA (0.5mM), followed by IB for RGS10, STIM1, STIM2, and CaM. **E)** RGS10 IP conducted as in (D) but in the absence of sodium deoxycholate. **F)** RGS10 IP from BV2 cells treated with vehicle or LPS (10 ng/mL) for 3 h, followed by IB for RGS10 and STIM2. All figures are representative of three independent experiments.

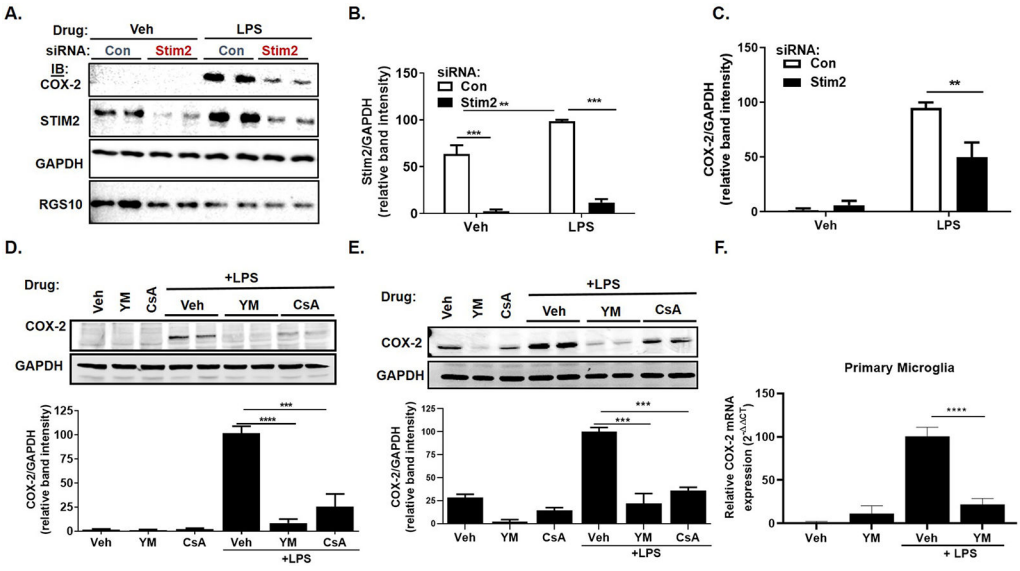

Figure 2. STIM2 and the Orai-calcineurin signaling axis are required for LPS-stimulated COX-2 expression.

A-C) BV2 cells were transfected with control siRNA (Con) or STIM2-targeted siRNA (Stim2). 24 hours after transfection, cells were treated with either serum-free media (Veh) or LPS (10 ng/mL) for additional 24 hours. **A)** Immunoblot (IB) of BV2 cells probed for COX-2, STIM2, RGS10, and GAPDH. **B)** Densitometry analysis of Stim2 data in (A) normalized to GAPDH. **C)** Normalized densitometry analysis of COX-2 data in (A). **D)** BV2 cells were pre-treated with Veh, or media containing either the Orai inhibitor YM58483 (YM) (10 uM) or the calcineurin inhibitor cyclosporin (CsA) (100 ng/mL) for 1 hour prior to a 24-hour incubation with Veh or LPS (10 ng/mL). COX-2 and GAPDH protein level was analyzed by IB (top panel), and quantified figures are shown (bottom panel). **E)** IB data of N9 cells treated as in (D), but with a modified LPS dose (100 ng/mL). **F)** Primary microglia isolated from postnatal mouse pups were pretreated with a Veh or YM (10 uM) for 1 hour, followed by treatment with Veh or LPS (10 ng/mL) for 24 h. Relative COX-2 mRNA expression analyzed by quantitative real-time PCR (qRT-PCR) normalized to an endogenous control β-actin ($2^{-\Delta\Delta Ct}$). qRT-PCR and western blot data were normalized to the lowest values, and representative data are presented as mean ± SEM pooled from three independent experiments. *p < 0.05, **p<0.01, and ***p<0.001, determined by one-way ANOVA followed by Tukey post hoc test.

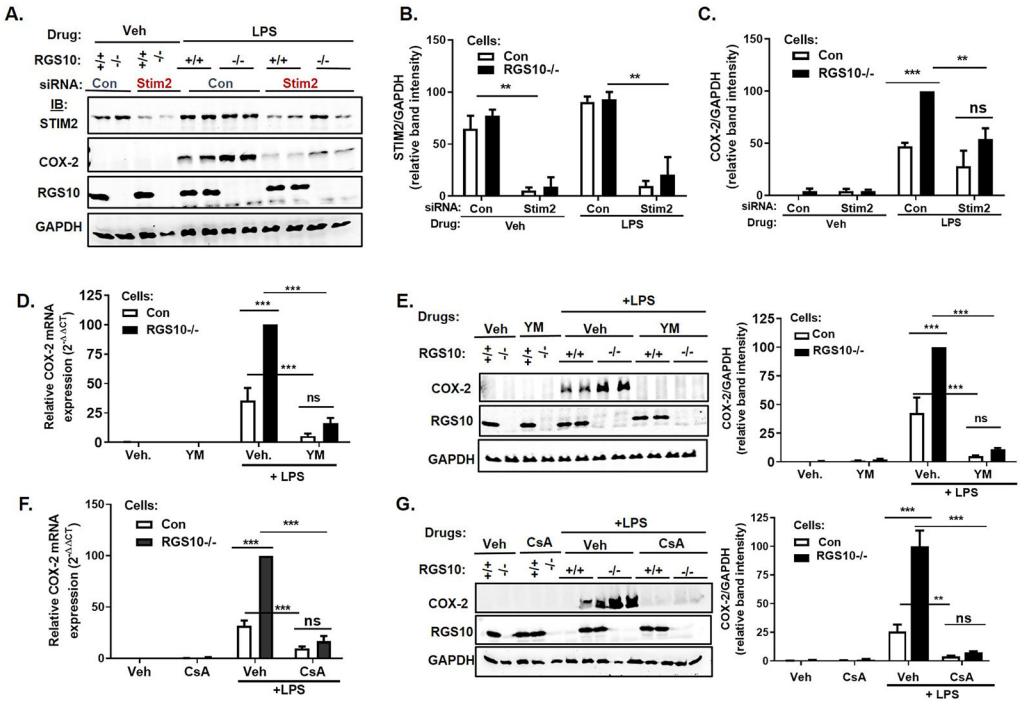

Figure 3. The STIM2-Orai-Calcineurin signaling axis mediates RGS10 sensitive COX-2 expression.

A-C) CRISPR-control (+/+) and RGS10 knockout (−/−) BV2 cells were transfected with control siRNA (Con) or STIM2-targeted siRNA (Stim2). 24 hours after transfection, cells were treated with either serum-free media (Veh) or LPS (10 ng/mL) for additional 24 hours. **A)** Immunoblot (IB) of BV2 cells probed for COX-2, STIM2, RGS10, and GAPDH. **B)** Densitometry analysis of Stim2 data in (A) normalized to GAPDH. **C)** Normalized densitometry analysis of COX-2 data in (A). **D-E)** Control and RGS10 knockout BV2 cells ($RGS10^{-/-}$) were treated with Veh or media containing 10 μM YM58483 (YM) for 1 hour prior to a 24-hour incubation with Veh or LPS (10 ng/mL). Relative COX-2 mRNA expression was analyzed by qRT-PCR **(D)**. IB of COX-2, RGS10, and GAPDH (left panel) and representative densitometry of COX-2 band intensity normalized to GAPDH (right panel) **(E). F-G)** Control and $RGS10^{-/-}$ cells treated with either Veh, 100ng/mL cyclosporine (CsA) and/or LPS (10 ng/mL) for 24 hours. Relative COX-2 mRNA expression was analyzed by qRT-PCR **(F)**. Representative IB images of COX-2, RGS10, and GAPDH (left panel) and densitometry of COX-2 band normalized to GAPDH (right panel) **(G)**. qRT-PCR data are normalized to endogenous control β-actin ($2^{-\Delta\Delta Ct}$). Fold difference of qRT-PCR and WB densitometry data were calculated after normalizing to a Veh treatment, and data represent mean ± SEM pooled from three independent experiments. *$p < 0.05$, **$p<0.01$, and ***$p<0.001$, determined by one-way ANOVA followed by Tukey post hoc test.

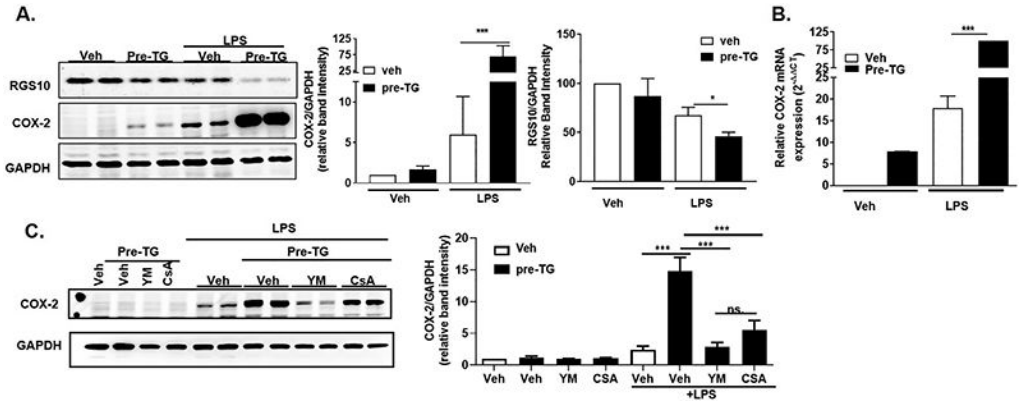

Figure 4. Depletion of calcium from intracellular stores amplifies LPS effects on COX-2 and RGS10 expression.

A-B) Wildtype BV2 cells were pretreated with vehicle or 1μM thapsigargin (TG) for 20 minutes. TG-containing media was removed and replaced by fresh media containing either vehicle or LPS (10 ng/mL) for 24 hours. **A).** Representative IB images of COX-2, RGS10, and GAPDH (left panel), and densitometry quantification (bar graphs). **B)** Relative COX-2 mRNA expression was analyzed by qRT-PCR. **C)** Representative IB images of COX-2 and GAPDH (left panel), and densitometry quantification (bar graph) of BV2 cells pretreated with TG as in (A-B) followed by LPS, alone or LPS in combination with either Orai inhibitor (YM) and calcineurin inhibitor (CsA). qRT-PCR data are normalized to endogenous control β-actin (2-ΔΔCt). Fold differences of qRT-PCR and WB densitometry data were calculated after normalizing to vehicle conditions, and data represent mean ± SEM pooled from three independent experiments. *$p < 0.05$, **$p<0.01$, and ***$p<0.001$, determined by one-way ANOVA followed by Tukey post hoc test.

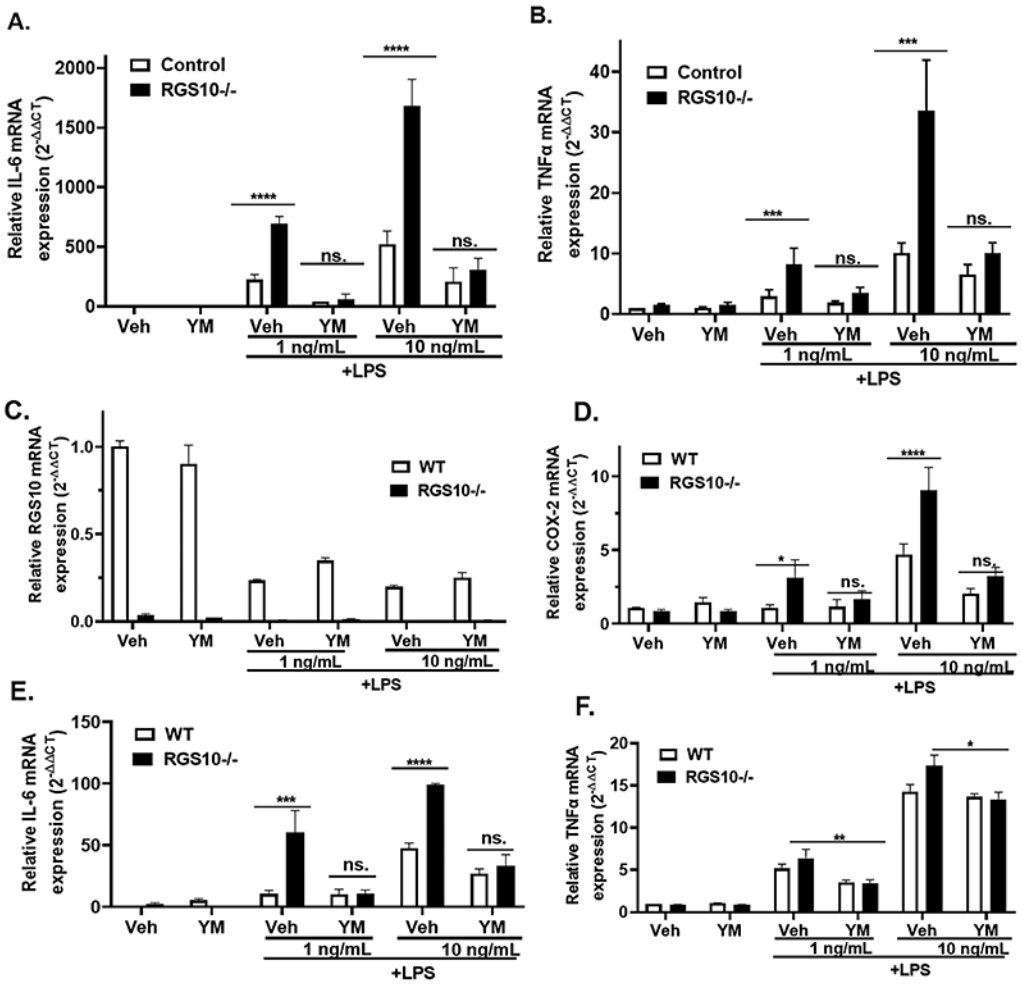

Figure 5. RGS10 requires SOCE to regulate LPS-induced pro-inflammatory genes in BV2 and primary microglia.

A&B) CRISPR-control (Control) and RGS10 knockout (RGS10−/−) BV2 cells were pretreated for 1 hour with serum-free medium (Veh) or the Orai inhibitor YM58483 (YM) (10 μM) prior to 24-hour incubation with Veh, LPS (1 ng/mL) or LPS (10 ng/mL). Relative expression of IL-6 transcript **(A)** and TNFα transcript **(B)** are analyzed by quantitative real-time PCR (qRT-PCR). **C-F)** Primary microglia from wild type (WT) and RGS10 knockout (RGS10−/−) mice were treated as in (A&B), and relative expression of RGS10 transcript (C), COX-2 transcript **(D)**, IL-6 transcript **(E)**, and TNFα transcript **(F)** are analyzed by qRT-PCR. Data are normalized to endogenous control β-actin ($2^{-\Delta\Delta Ct}$) and fold differences are calculated after normalizing to vehicle treatment groups. Data represent mean ± SEM pooled from 7-8 experiments for BV2 cells (A-C) and three experiments for primary microglia (D-G). *p < 0.05, **p<0.01, and ***p<0.001, determined by one-way ANOVA followed by Tukey post hoc test.

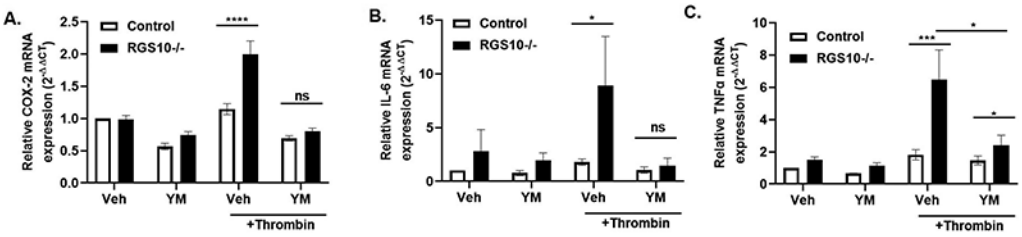

Figure 6. Loss of RGS10 upregulates thrombin-stimulated pro-inflammatory genes in BV2 microglia in SOCE-dependent mechanism.

CRISPR-control (Control) and RGS10 knockout (RGS10−/−) BV2 cells were treated with Fatty acid-free BSA (Veh) or Thrombin (10 U/mL) for 4 hours with or without a 1-hour pretreatment with Orai inhibitor YM58483 (YM) (10 μM). Relative expression of COX-2 transcript (**A**), IL-6 transcript (**B**), and TNFα transcript (**C**) are analyzed by qRT-PCR. Data are normalized to endogenous control β-actin ($2^{-\Delta\Delta Ct}$) and fold difference is calculated after normalizing to the vehicle treatment group of control cells. Represented data are mean ± SEM pooled from 4-5 independent experiments. *$p < 0.05$, **$p<0.01$, and ***$p<0.001$, determined by ANOVA followed by Tukey post hoc test.

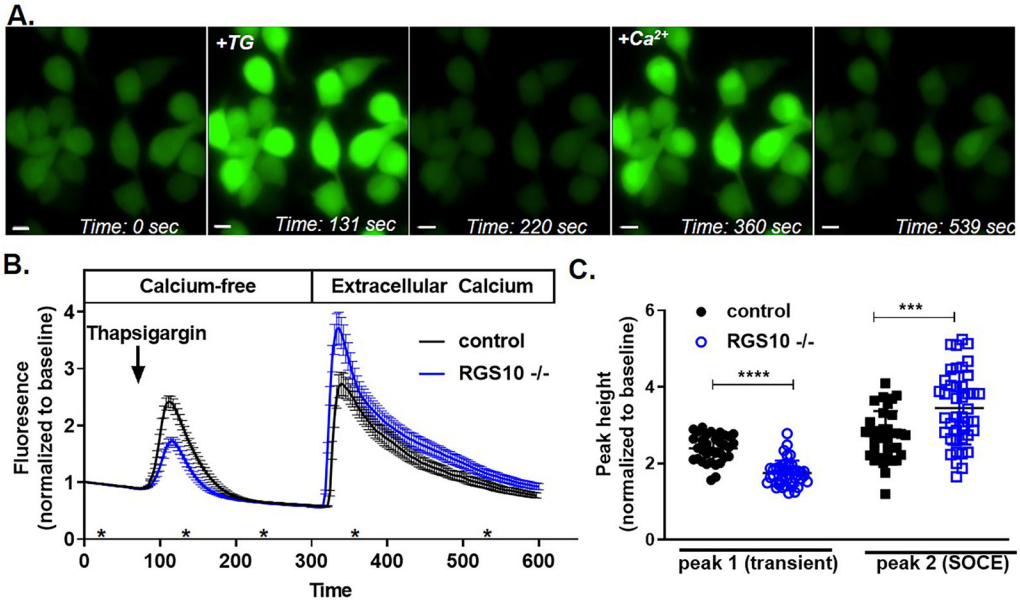

Figure 7. Loss of RGS10 enhances store-operated calcium entry (SOCE) triggered by ER depletion.

BV2 cells were loaded with 5 μM CAL520-AM for 20 min at 37°C and incubated in calcium-free buffer containing EGTA. Live cell imaging was initiated at time=0, and TG (1 μM) and Ca^{2+} (1.8 mM) were added at 60 sec and 300 sec, respectively. Images were captured every 3 sec. **A)** Representative fluorescence images of control BV2 cells at indicated time points. **B)** Quantified tracings of average fluorescence intensity in CRISPR-control BV2 cells (black) and RGS10 knockout BV2 cells (blue). Error bars indicate standard deviation from at least ten cells in a single experiment. Asterisks (*) indicate approximate time points corresponding to images shown in (A). **C)** Average peak height of the TG-induced Ca^{2+} transient calcium signal and SOCE signal observed after 1.8 mM Ca^{2+} addition, from three independent experiments, with 10-15 cells quantified from each cell line in each experiment. *$p < 0.05$, **$p<0.01$, and ***$p<0.001$, determined by unpaired student's t-test.

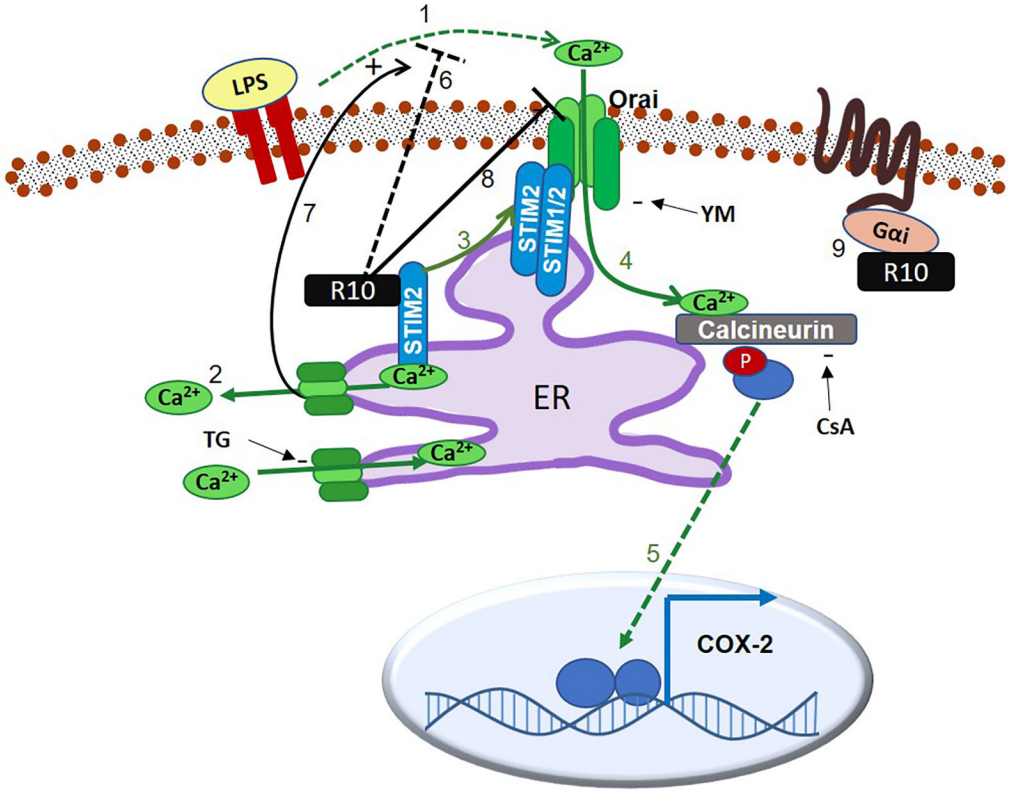

Figure 8. Model and Summary: RGS10 regulates pro-inflammatory gene expression through functional interaction with the SOCE machinery.

LPS facilitates extracellular calcium entry through plasma membrane Orai channels, a mechanism known as store-operated calcium entry (SOCE) (1). SOCE is activated through an upstream mechanism involving calcium depletion from intracellular stores. Upon ER depletion (2), calcium dissociates from the ER membrane resident calcium sensor STIM2, triggering STIM2 translocation to ER-PM junctions where it forms a complex with STIM1 and Orai subunits to form an active calcium channel (3). SOCE through Orai is tightly coupled to activation of the phosphatase calcineurin (4), which triggers activation of downstream substrates and promotes the expression of pro-inflammatory genes (5). Our data demonstrate that LPS requires an intact SOCE pathway including STIM2, Orai, and calcineurin to trigger pro-inflammatory gene expression through undefined, indirect mechanisms. We previously showed that RGS10 (R10) suppresses LPS-induced pro-inflammatory gene expression in a G-protein independent mechanism. Here, we show that RGS10 selectively interacts with STIM2, and RGS10-mediated regulation of LPS response requires activation of the STIM2-Orai-Calcineurin pathway (6). Depletion of intracellular calcium (2) activates SOCE and enhances LPS response (7), and RGS10 suppresses SOCE triggered by store depletion (8). In addition to G protein-independent regulation of LPS response, RGS10 also mediates signaling in microglia through its canonical interaction with Gαi subunits (9). The interplay of RGS10 co-regulation of these two critical pathways and the specific role of RGS10-STIM2 biochemical interaction is unknown. It is plausible that RGS10 regulates SOCE and downstream pro-inflammatory response by interacting with and/or modulating STIIM2 function such as STIM2 activation, PM translocation, and

interaction with STIM1/Orai channel (3). Similar to the regulation of TLR4 response, RGS10 also suppresses thrombin-stimulated pro-inflammatory genes through a mechanism requiring Orai activity, suggesting that RGS10 has the potential to regulate a broad range of inflammatory responses that depend on SOCE. The effects of pharmacological agents Thapsigargin (TG), YM58483 (YM), and cyclosporine A (CsA) are shown.